

**SURVEY AND LOGISTICS REPORT
ON A HELICOPTER BORNE
VERSATILE TIME DOMAIN
ELECTROMAGNETIC (VTEM)
SURVEY**

on the

AVEBURY, TASMANIA AREA

AUSTRALIA

for

MINERALS AND METALS GROUP

by



GEOTECH AIRBORNE PTY LTD

Unit 1, 29 Mulgul Road
Malaga, WA, 6090,
Australia
Tel: +61 8 9249 8814
Fax: +61 8 9249 8894
www.geotechairborne.com
e-mail: info@geotechairborne.com

**Project AA901
February, 2011**

TABLE OF CONTENTS

| | |
|--|----|
| 1. SURVEY SPECIFICATIONS | 3 |
| 1.1. General | 3 |
| 1.2. VTEM flight plan on Google EARTH™ Background | 3 |
| 1.3. Survey block coordinates. | 4 |
| 1.4. Survey block specifications | 4 |
| 1.5. Survey schedule | 4 |
| 2. SYSTEM SPECIFICATIONS | 5 |
| 2.1. Instrumentation | 5 |
| 2.2. VTEM Configuration | 6 |
| 2.3. VTEM decay sampling scheme | 6 |
| 2.4. VTEM Transmitter Waveform over one half-period (January 2011) | 7 |
| 3. PROCESSING | 8 |
| 3.1. Processing parameters..... | 8 |
| 3.2. Flight Path..... | 8 |
| 3.3. Electromagnetic Data | 8 |
| 3.4. Magnetic Data | 8 |
| 3.5. Digital Terrain Model | 9 |
| 4. DELIVERABLES | 10 |
| 5. PERSONNEL..... | 12 |

APPENDICES

| | |
|------------------------------------|-----------|
| A. Modeling VTEM data | 13 |
| B. Geophysical Maps | 19 |



SURVEY AND LOGISTICS REPORT ON A HELICOPTER-BORNE VTEM SURVEY

1. SURVEY SPECIFICATIONS

1.1. General

| | |
|-----------------------|---|
| Job Number | AA901 |
| Client | Minerals and Metals Group. |
| Project Area | Avebury, Tasmania Area |
| Location | Australia |
| Number of Blocks | 1 |
| Total line kilometres | 423 |
| Survey date | 12 - 20 January, 2011 |
| Client Representative | Neil Hughes Tel: +61 3 9288 0759 Fax: +61 3 9288 0800 neil.hughes@mmgrouppltd.com |
| Client address | Level 23, 28 Freshwater Place Southbank, Victoria, 3006, Australia |

1.2. VTEM flight plan on Google EARTH™ Background



1.3. Survey block coordinates.

| Easting UTM Z 55S | Northing UTM Z 55S |
|-------------------|--------------------|
| Avebury Area | |
| 354124.86 | 5360186.15 |
| 354124.86 | 5358161.11 |
| 352111.47 | 5358161.11 |
| 352111.47 | 5357171.86 |
| 348142.86 | 5357171.86 |
| 348142.86 | 5356706.34 |
| 349690.73 | 5355181.74 |
| 351110.59 | 5355181.74 |
| 351110.59 | 5354180.86 |
| 352111.47 | 5354180.86 |
| 352111.47 | 5353179.98 |
| 356114.99 | 5353179.98 |
| 356114.99 | 5357183.50 |
| 357115.87 | 5357183.50 |
| 357115.87 | 5358184.39 |
| 356114.99 | 5358184.39 |
| 356114.99 | 5360186.15 |

1.4. Survey block specifications

| Survey block | Line spacing (m) | Line-km (contractual) | Line-km (delivered) | Flight direction | Line number |
|--------------|------------------|-----------------------|---------------------|------------------|-----------------|
| Avebury | 100 | 500 | 423 | 000 – 180 | L10010 – L10900 |
| | 1500 | | | 090 – 270 | T90010 – T90050 |

1.5. Survey schedule

| Date | Flight # | Block | Nominal Production Km flown | Comments |
|-----------|----------|---------|-----------------------------|-------------|
| 12-Jan-11 | 1 | Avebury | N/A | Test Flight |
| 16-Jan-11 | 2,3 | Avebury | 209 | Production |
| 20-Jan-11 | 4,5 | Avebury | 216 | Production |



2. SYSTEM SPECIFICATIONS

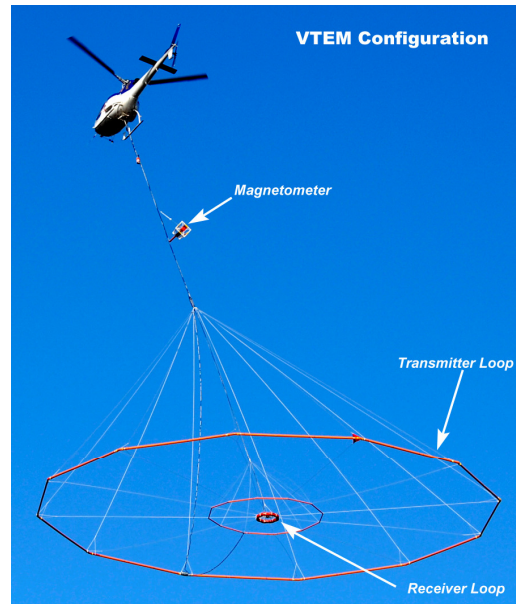
2.1. Instrumentation

| Survey Helicopter | |
|-------------------------------|--------------------------------|
| Model | AS 350 B3 |
| Registration | VH-VTX |
| Nominal survey speed | 80 km/h |
| Nominal terrain clearance | 75 m |
| VTEM Transmitter | |
| Coil diameter | 26 m |
| Number of turns | 4 |
| Pulse repetition rate | 25 Hz |
| Peak current | 200 Amp |
| Duty cycle | 42% |
| Peak dipole moment | 425,000 NIA |
| Pulse width | 8.34 ms |
| Nominal terrain clearance | 41 m |
| VTEM Receiver | |
| Coil diameter | 1.2 metre |
| Number of turns | 100 |
| Effective area | 113.1 m ² |
| Sampling interval | 0.1 s |
| Nominal terrain clearance | 41 m |
| Magnetometer | |
| Type | Geometrics |
| Model | Optically pumped cesium vapour |
| Sensitivity | 0.02 nT |
| Sampling interval | 0.1 s |
| Cable length | 12 m |
| Nominal terrain clearance | 65 m |
| Radar Altimeter | |
| Type | Terra TRA 3000/TRI 40 |
| Position | Beneath cockpit |
| Sampling interval | 0.2 s |
| GPS navigation system | |
| Type | NovAtel |
| Model | WAAS enabled OEM4-G2-3151W |
| Antenna position | Helicopter tail |
| Sampling interval | 0.2 s |
| Base Station Magnetometer/GPS | |
| Type | Geometrics |
| Model | Cesium vapour |
| Sensitivity | 0.001 nT |
| Sampling interval | 1 s |



2.2. VTEM Configuration

| Configuration | |
|-----------------------------|------|
| Cable angle with vertical | 35 ° |
| Cable length (EM receiver) | 42 m |
| Cable length (Magnetometer) | 12 m |

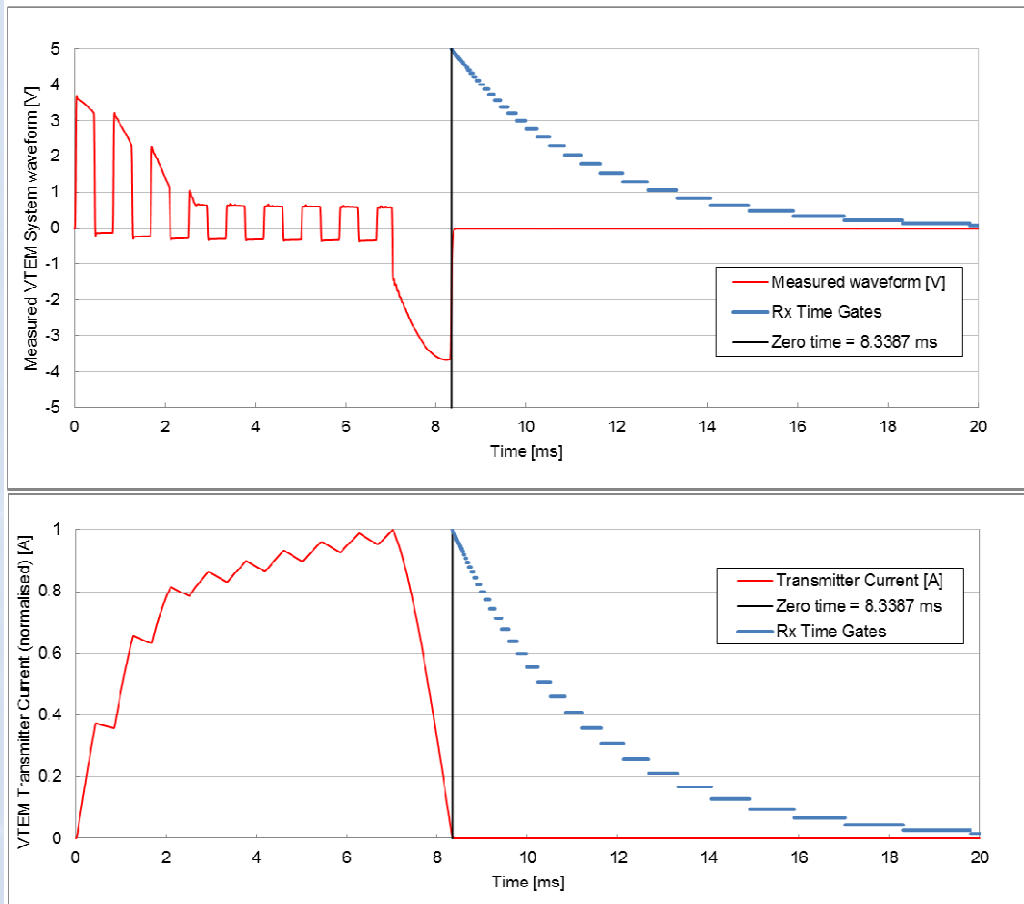


2.3. VTEM decay sampling scheme

| B-field VTEM Decay Sampling scheme | | | | |
|------------------------------------|--------------|-------|------|-------|
| Array | Microseconds | | | |
| Index | Middle | Start | End | Width |
| 13 | 83 | 78 | 90 | 12 |
| 14 | 96 | 90 | 103 | 13 |
| 15 | 110 | 103 | 118 | 15 |
| 16 | 126 | 118 | 136 | 18 |
| 17 | 145 | 136 | 156 | 20 |
| 18 | 167 | 156 | 179 | 23 |
| 19 | 192 | 179 | 206 | 27 |
| 20 | 220 | 206 | 236 | 30 |
| 21 | 253 | 236 | 271 | 35 |
| 22 | 290 | 271 | 312 | 40 |
| 23 | 333 | 312 | 358 | 46 |
| 24 | 383 | 358 | 411 | 53 |
| 25 | 440 | 411 | 472 | 61 |
| 26 | 505 | 472 | 543 | 70 |
| 27 | 580 | 543 | 623 | 81 |
| 28 | 667 | 623 | 716 | 93 |
| 29 | 766 | 716 | 823 | 107 |
| 30 | 880 | 823 | 945 | 122 |
| 31 | 1010 | 945 | 1086 | 141 |
| 32 | 1161 | 1086 | 1247 | 161 |
| 33 | 1333 | 1247 | 1432 | 185 |
| 34 | 1531 | 1432 | 1646 | 214 |
| 35 | 1760 | 1646 | 1891 | 245 |
| 36 | 2021 | 1891 | 2172 | 281 |
| 37 | 2323 | 2172 | 2495 | 323 |
| 38 | 2667 | 2495 | 2865 | 370 |
| 39 | 3063 | 2865 | 3292 | 427 |
| 40 | 3521 | 3292 | 3781 | 490 |
| 41 | 4042 | 3781 | 4341 | 560 |
| 42 | 4641 | 4341 | 4987 | 646 |
| 43 | 5333 | 4987 | 5729 | 742 |
| 44 | 6125 | 5729 | 6581 | 852 |
| 45 | 7036 | 6581 | 7560 | 979 |
| 46 | 8083 | 7560 | 8685 | 1125 |
| 47 | 9286 | 8685 | 9977 | 1292 |



2.4. VTEM Transmitter Waveform over one half-period (January 2011)



3. PROCESSING

3.1. Processing parameters

| Coordinates | |
|---|----------------------|
| Projection | MAP GRID AUS ZONE 55 |
| Datum | GDA 94 |
| | |
| Spherics rejection (EM and Magnetic data) | |
| Non-linear filter | 4 point |
| Non-linear filter sensitivity | 0.0001 |
| Low-pass filter wavelength | 20 fids |
| | |
| Lag correction of other sensors to EM receiver position | |
| GPS | 16 m |
| Radar | 26 m |
| Magnetometer | 17 m |

3.2. Flight Path

The flight path, recorded by the acquisition program as WGS 84 latitude/longitude, was converted into the UTM coordinate system in Oasis Montaj. The flight path was drawn using linear interpolation between x,y positions from the navigation system. Positions are updated every second and expressed as UTM eastings (x) and UTM northings (y).

3.3. Electromagnetic Data

A three stage digital filtering process was used to reject major spheric events and to reduce system noise. Local spheric activity can produce sharp, large amplitude events that cannot be removed by conventional filtering procedures. Smoothing or stacking will reduce their amplitude but leave a broader residual response that can be confused with geological phenomena. To avoid this possibility, a computer algorithm searches out and rejects the major spheric events.

The signal to noise ratio was further improved by the application of a low pass linear digital filter. This filter has zero phase shift which prevents any lag or peak displacement from occurring, and it suppresses only variations with a wavelength less than the specified filter wavelength.

3.4. Magnetic Data

The processing of the magnetic data involved the correction for diurnal variations by using the digitally recorded ground base station magnetic values. The base station magnetometer data was edited and merged into the Geosoft GDB database on a daily basis. The aeromagnetic data was corrected for diurnal variations by subtracting the observed magnetic base station deviations.

Tie line levelling was carried out by adjusting intersection points along the traverse lines. A micro-levelling procedure was then applied. This technique is designed to remove persistent low-amplitude components of flight-line noise remaining after tie line levelling.

The corrected magnetic data was interpolated between survey lines using a random point gridding method to yield x-y grid values for a standard grid cell size of a quarter of the line spacing. The Minimum Curvature algorithm was used to interpolate values onto a rectangular regular spaced grid.



3.5. Digital Terrain Model

Subtracting the radar altimeter data from the GPS elevation data creates a digital elevation model.



4. DELIVERABLES

| VTEM Survey and logistics report | | |
|----------------------------------|---|---|
| Format | PDF | |
| Copies | 2 x Digital (DVD/CD) 2 x Hard copy | |
| Database | | |
| Format | Digital Geosoft (.GDB) | |
| Channels | Name | Description |
| | X_UTM | X positional data (UTM Z55S / WGS84) |
| | Y_UTM | Y positional data (UTM Z55S / WGS84) |
| | X_MGA | X positional data (MGA Z55 / GDA94) |
| | Y_MGA | Y positional data (MGA Z55 / GDA94) |
| | Lon | Longitude data |
| | Lat | Latitude data |
| | Z | GPS antenna elevation (metres above sea level) |
| | Radar | Helicopter terrain clearance from radar altimeter (metres above ground level) |
| | RxAlt | EM Receiver and Transmitter terrain clearance (metres above ground level) |
| | DTM | Digital terrain model (metres) |
| | Gtime | UTC time (seconds of the day) |
| | MagTF | Raw Total Magnetic field data (nT) |
| | MagBase | Magnetic diurnal variation data (nT) |
| | MagDiu | Total Magnetic field diurnal variation and lag corrected data (nT) |
| | MagTieL | Tie-line leveled Total Magnetic field data (nT) |
| | MagMicL | Microleveled Total Magnetic field data (nT) |
| | dBdtZ[13] to dBdtZ[47] | dB/dtZ, Time Gates 83 μ s to 9286 μ s (μ V/A/m ⁴) |
| BfieldZ[13] to BfieldZ[47] | BfieldZ, Time Gates 83 μ s to 9286 μ s (μ V*m/A/m ⁴) | |
| PLM | Power line monitor | |

| Grids | | |
|--------|---|---------------------------|
| Format | Digital Geosoft (.GRD and .GI) ¹ | |
| Grids | Name | Description |
| | AA901_Mag | Total Magnetic field (nT) |

| Maps | | |
|--------|------------------------|--|
| Format | Digital Geosoft (.MAP) | |
| Scale | 1:10 000 | |
| Maps | Name | Description |
| | AA901_Mag | Total Magnetic field colour contours |
| | AA901_dBdtZ_Log | VTEM dB/dt profiles, Time Gates 0.667 – 9.286 ms in linear - logarithmic scale |
| | AA901_BfieldZ_Log | VTEM B-field profiles, Time Gates 0.667 – 9.286 ms in linear - logarithmic scale |

¹ A Geosoft .GRD file has a .GI metadata file associated with it, containing grid projection information.



| Waveform | | |
|----------|---|---|
| Format | Digital Excel Spreadsheet (AA901_VTEM_Waveform.xls) | |
| Columns | Name | Description |
| | Time | Sampling rate interval, 5.208 μ s |
| | Volt | Output voltage of the receiver coil (volt) |
| | Current | Transmitter current (normalised to 1A peak) |

| Google Earth Flight Path file | |
|-------------------------------|---|
| Format | Google Earth AA901_FlightPath.kml |
| | Free version of Google Earth software can be downloaded from, http://earth.google.com/download-earth.html |



5. PERSONNEL

| Geotech Airborne Limited Personnel | |
|------------------------------------|--|
| Operator / Crew chief | Victor Wijaya |
| Data Processing (Preliminary) | Pete Holbrook |
| Data Processing (Final) /Reporting | Matt Holbrook |
| Final data supervision | Malcolm Moreton Data Processing Manager (malcolm@geotechairborne.com) |
| Overall project management | Keith Fisk Managing Partner and Director (keith@geotechairborne.com) |



APPENDIX A

GENERALIZED MODELING RESULTS OF THE VTEM SYSTEM (by Roger Barlow)

Introduction

The VTEM system is based on a concentric or central loop design, whereby, the receiver is positioned at the centre of a 26.1 metres diameter transmitter loop that produces a dipole moment up to 625,000 NIA at peak current. The wave form is a bi-polar, modified square wave with a turn-on and turn-off at each end. With a base frequency of 25 Hz, the duration of each pulse is approximately 7.5 milliseconds followed by an off time where no primary field is present.

During turn-on and turn-off, a time varying field is produced (dB/dt) and an electromotive force (emf) is created as a finite impulse response. A current ring around the transmitter loop moves outward and downward as time progresses. When conductive rocks and mineralization are encountered, a secondary field is created by mutual induction and measured by the receiver at the centre of the transmitter loop.

Measurements are made during the off-time, when only the secondary field (representing the conductive targets encountered in the ground) is present.

Efficient modeling of the results can be carried out on regularly shaped geometries, thus yielding close approximations to the parameters of the measured targets. The following is a description of a series of common models made for the purpose of promoting a general understanding of the measured results.

Variation of Plate Depth

Geometries represented by plates of different strike length, depth extent, dip, plunge and depth below surface can be varied with characteristic parameters like conductance of the target, conductance of the host and conductivity/thickness and thickness of the overburden layer.

Diagrammatic models for a vertical plate are shown in figures A and G at two different depths, all other parameters remaining constant. With this transmitter-receiver geometry, the classic **M** shaped response is generated. Figure A shows a plate where the top is near surface. Here, amplitudes of the dual peaks are higher and symmetrical with the zero centre positioned directly above the plate. Most important is the separation distance of the peaks. This distance is small when the plate is near surface and widens with a linear relationship as the plate (depth to top) increases. Figure G shows a much deeper plate where the separation distance of the peaks is much wider and the amplitudes of the channels have decreased.

Variation of Plate Dip

As the plate dips and departs from the vertical position, the peaks become asymmetrical. Figure B shows a near surface plate dipping 80°. Note that the direction of dip is toward the high shoulder of the response and the top of the plate remains under the centre minimum.

As the dip increases, the aspect ratio (Min/Max) decreases and this aspect ratio can be used as an empirical guide to dip angles from near 90° to about 30°. The method is not sensitive enough where dips are less than about 30°. Figure E shows a plate dipping 45° and, at this angle, the minimum shoulder starts to vanish. In Figure D, a



flat lying plate is shown, relatively near surface. Note that the twin peak anomaly has been replaced by a symmetrical shape with large, bell shaped, channel amplitudes which decay relative to the conductance of the plate.

Figure H shows a special case where two plates are positioned to represent a synclinal structure. Note that the main characteristic to remember is the centre amplitudes are higher (approximately double) compared to the high shoulder of a single plate. This model is very representative of tightly folded formations where the conductors were once flat lying.

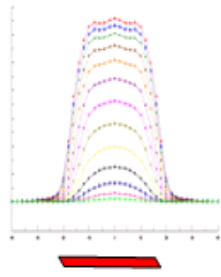
Variation of Prism Depth

Finally, with prism models, another algorithm is required to represent current on the plate. A plate model is considered to be infinitely thin with respect to thickness and incapable of representing the current in the thickness dimension. A prism model is constructed to deal with this problem, thereby, representing the thickness of the body more accurately.

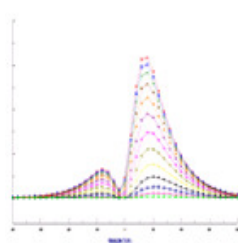
Figures C, F and I show the same prism at increasing depths. Aside from an expected decrease in amplitude, the side lobes of the anomaly show a widening with deeper prism depths of the bell shaped early time channels.



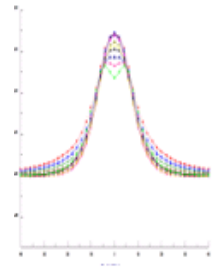
A



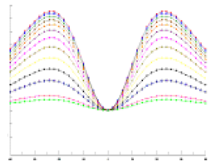
B



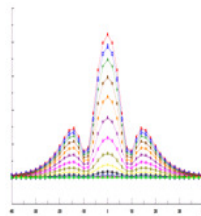
C



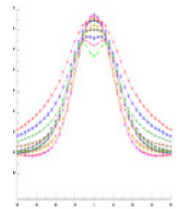
D



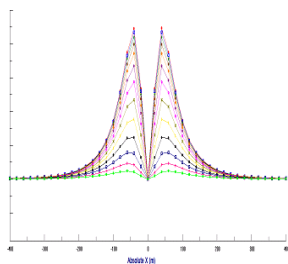
E



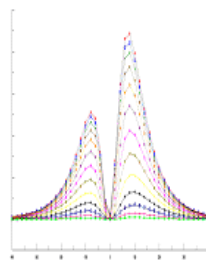
F



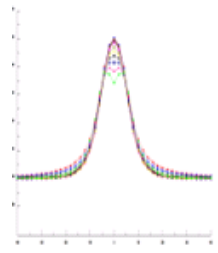
G



H



I



General Modeling Concepts

A set of models has been produced for the Geotech VTEM[®] system with explanation notes (see models A to I above). The reader is encouraged to review these models, so as to get a general understanding of the responses as they apply to survey results. While these models do not begin to cover all possibilities, they give a general perspective on the simple and most commonly encountered anomalies.

When producing these models, a few key points were observed and are worth noting as follows:

- For near vertical and vertical plate models, the top of the conductor is always located directly under the centre low point between the two shoulders in the classic **M** shaped response.
- As the plate is positioned at an increasing depth to the top, the shoulders of the **M** shaped response, have a greater separation distance.
- When faced with choosing between a flat lying plate and a prism model to represent the target (broad response) some ambiguity is present and caution should be exercised.
- With the concentric loop system and Z-component receiver coil, virtually all types of conductors and most geometries are most always well coupled and a response is generated (see model H). Only concentric loop systems can map this type of target.

The modelling program used to generate the responses was prepared by PetRos Eikon Inc. and is one of a very few that can model a wide range of targets in a conductive half space.

General Interpretation Principals

Magnetics

The total magnetic intensity responses reflect major changes in the magnetite and/or other magnetic minerals content in the underlying rocks and unconsolidated overburden. Precambrian rocks have often been subjected to intense heat and pressure during structural and metamorphic events in their history. Original signatures imprinted on these rocks at the time of formation have, in most cases, been modified, resulting in low magnetic susceptibility values.

The amplitude of magnetic anomalies, relative to the regional background, helps to assist in identifying specific magnetic and non-magnetic rock units (and conductors) related to, for example, mafic flows, mafic to ultramafic intrusives, felsic intrusives, felsic volcanics and/or sediments etc. Obviously, several geological sources can produce the same magnetic response. These ambiguities can be reduced considerably if basic geological information on the area is available to the geophysical interpreter.



In addition to simple amplitude variations, the shape of the response expressed in the wave length and the symmetry or asymmetry, is used to estimate the depth, geometric parameters and magnetization of the anomaly. For example, long narrow magnetic linears usually reflect mafic flows or intrusive dyke features. Large areas with complex magnetic patterns may be produced by intrusive bodies with significant magnetization, flat lying magnetic sills or sedimentary iron formation. Local isolated circular magnetic patterns often represent plug-like igneous intrusives such as kimberlites, pegmatites or volcanic vent areas.

Because the total magnetic intensity (TMI) responses may represent two or more closely spaced bodies within a response, the second derivative of the TMI response may be helpful for distinguishing these complexities. The second derivative is most useful in mapping near surface linears and other subtle magnetic structures that are partially masked by nearby higher amplitude magnetic features. The broad zones of higher magnetic amplitude, however, are severely attenuated in the vertical derivative results. These higher amplitude zones reflect rock units having strong magnetic susceptibility signatures. For this reason, both the TMI and the second derivative maps should be evaluated together.

Theoretically, the second derivative, zero contour or colour delineates the contacts or limits of large sources with near vertical dip and shallow depth to the top. The vertical gradient map also aids in determining contact zones between rocks with a susceptibility contrast, however, different, more complicated rules of thumb apply.

Concentric Loop EM Systems

Concentric systems with horizontal transmitter and receiver antennae produce much larger responses for flat lying conductors as contrasted with vertical plate-like conductors. The amount of current developing on the flat upper surface of targets having a substantial area in this dimension, are the direct result of the effective coupling angle, between the primary magnetic field and the flat surface area. One therefore, must not compare the amplitude/conductance of responses generated from flat lying bodies with those derived from near vertical plates; their ratios will be quite different for similar conductances.

Determining dip angle is very accurate for plates with dip angles greater than 30°. For angles less than 30° to 0°, the sensitivity is low and dips can not be distinguished accurately in the presence of normal survey noise levels.

A plate like body that has near vertical position will display a two shoulder, classic **M** shaped response with a distinctive separation distance between peaks for a given depth to top.

It is sometimes difficult to distinguish between responses associated with the edge effects of flat lying conductors and poorly conductive bedrock conductors. Poorly conductive bedrock conductors having low dip angles will also exhibit responses that may be interpreted as surficial overburden conductors. In some situations, the conductive response has line to line continuity and some magnetic correlation providing possible evidence that the response is related to an actual bedrock source.

The EM interpretation process used, places considerable emphasis on determining an understanding of the general conductive patterns in the area of interest. Each area has different characteristics and these can effectively guide the detailed process used.



The first stage is to determine which time gates are most descriptive of the overall conductance patterns. Maps of the time gates that represent the range of responses can be very informative.

Next, stacking the relevant channels as profiles on the flight path together with the second vertical derivative of the TMI is very helpful in revealing correlations between the EM and Magnetics.

Next, key lines can be profiled as single lines to emphasize specific characteristics of a conductor or the relationship of one conductor to another on the same line. Resistivity Depth sections can be constructed to show the relationship of conductive overburden or conductive bedrock with the conductive anomaly.



APPENDIX B
GEOPHYSICAL MAP IMAGES
(not to scale)



